Physics Letters B 787 (2018) 198–203

Contents lists available at ScienceDirect

Physics Letters B

www.elsevier.com/locate/physletb

Lifetime measurement of the 2_1^+ state in ^{74}Rb and isospin properties of quadrupole transition strengths at $N = Z$

C. Morse [a,b,d,*,1], H. Iwasaki [a,b], A. Lemasson [a], A. Dewald [c], T. Braunroth [c], V.M. Bader [a,b], T. Baugher [a,b], D. Bazin [a], J.S. Berryman [a], C.M. Campbell [d], A. Gade [a,b], C. Langer [a,e], I.Y. Lee [d], C. Loelius [a,b], E. Lunderberg [a,b], F. Recchia [a], D. Smalley [a], S.R. Stroberg [a,b], R. Wadsworth [f], C. Walz [a,g], D. Weisshaar [a], A. Westerberg [h], K. Whitmore [a,b], K. Wimmer [a,h]

[a] National Superconducting Cyclotron Laboratory, Michigan State University, East Lansing, MI 48824, USA
[b] Department of Physics and Astronomy, Michigan State University, East Lansing, MI 48824, USA
[c] Institut für Kernphysik der Universität zu Köln, D-50937 Köln, Germany
[d] Nuclear Science Division, Lawrence Berkeley National Laboratory, Berkeley, CA 94720, USA
[e] Joint Institute for Nuclear Astrophysics, Michigan State University, East Lansing, MI 48824, USA
[f] Department of Physics, University of York, Heslington, York YO10 5DD, United Kingdom
[g] Institut für Kernphysik, Technische Universität Darmstadt, 64289 Darmstadt, Germany
[h] Department of Physics, Central Michigan University, Mount Pleasant, MI 48859, USA

ARTICLE INFO

Article history:
Received 16 August 2018
Received in revised form 19 September 2018
Accepted 1 October 2018
Available online 8 November 2018
Editor: D.F. Geesaman

Keywords:
Lifetimes
Nuclear transition probabilities
Isospin

ABSTRACT

Self-conjugate nuclei in the $A \approx 70$–80 region have attracted a great deal of attention due to phenomena such as shape coexistence and increasing collectivity along the $N = Z$ line. We investigate the structure of nuclei in this region through lifetime measurements using the GRETINA array. The first implementation of the Differential Recoil Distance Doppler Shift technique with fast radioactive beams is demonstrated and verified through a measurement of the well-known $B(E2; 2_1^+ \rightarrow 0_1^+)$ transition strength in ^{74}Kr. The method is then applied to determine the $B(E2; 2_1^+ \rightarrow 0_1^+)$ transition strength in ^{74}Rb, the heaviest odd–odd $N = Z$ nucleus for which this quantity has been determined. This result and extended systematics along $N = Z$ suggest the dominance of the isoscalar part of the quadrupole transition strengths in self-conjugate nuclei, as well as the possible presence of shape coexistence in ^{74}Rb.

1. Introduction

Nuclei along the $N = Z$ line offer a unique opportunity to study nuclear structure. Being symmetric with respect to the isospin degree of freedom, these systems offer an ideal setting in which to study isospin symmetry breaking effects, for example through the differences in the excitation energies of isobaric analogue states in an isospin multiplet [1]. The odd–odd $N = Z$ nuclei are particularly interesting in this regard, as a competition can arise between the isoscalar ($T = 0$) and isovector ($T = 1$) pairing modes. These nuclei are also host to many of the most precisely measured superallowed Fermi β decay strengths available, which provide important tests of predictions for the electroweak interaction such as the CVC hypothesis and the unitarity of the CKM matrix [2]. Such tests rely on accurate knowledge of the wave function of the nuclear states involved in the transitions, and so information regarding the structure of these nuclei provides an important input for fundamental physics.

The nuclei near the $N = Z$ line in the vicinity of mass $A \approx 70$ exhibit a particularly wide variety of nuclear structure phenomena. These nuclear systems evolve very rapidly as a function of both nucleon number and angular momentum; nuclei in this region have been observed to transition through many different shapes along the $N = Z$ line as well as along isotopic chains [3–7]. This has been understood as a consequence of the many gaps between the Nilsson levels which stabilize different shapes at similar particle numbers [8]. For $N \approx Z$ nuclei, where protons and neutrons

* Corresponding author at: Nuclear Science Division, Lawrence Berkeley National Laboratory, Berkeley, CA 94720, USA.
E-mail address: cmorse@lbl.gov (C. Morse).
[1] Present address: Nuclear Science Division, Lawrence Berkeley National Laboratory, Berkeley, CA 94720, USA.

https://doi.org/10.1016/j.physletb.2018.10.064

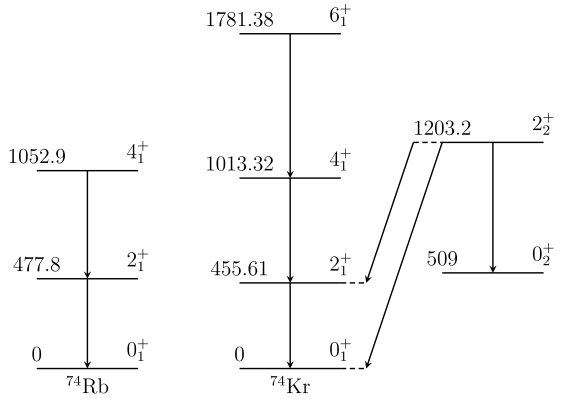

Fig. 1. A partial level scheme of the lowest-lying levels in ^{74}Rb and ^{74}Kr, with level energies given in keV. The isobaric analogue states in the yrast bands of both nuclei can be clearly identified. Data for ^{74}Rb are from [20], while data for ^{74}Kr are from [21].

are filling the same orbitals, this can give rise to coexisting structures with different intrinsic deformations, i.e. shape coexistence. This has been observed in ^{68,72}Se [9,10] as well as the proton-rich krypton isotopes near $N = Z$ [7]. Such phenomena make this area of the nuclear chart an attractive location to investigate nuclear structure and to test the predictions of nuclear models.

Despite the rich diversity of nuclear structure in this region, the $N \approx Z$ nuclei near $A \approx 70 - 80$ have proven challenging to study. This is due in part to the fact that it is difficult to produce rare-isotope beams of these nuclei with sufficient purity and intensity, as well as the large computational effort that is required for theoretical calculations. Of particular relevance for understanding the structure of the nuclei in this region are the $B(E2; 2_1^+ \rightarrow 0_1^+)$ transition rates, which provide an important measure of the collectivity of the nucleus. The even–even nuclei have fared relatively well in this regard, as the $B(E2)$ strengths along the $N = Z$ line have been measured up to ^{76}Sr [11]. The odd–odd nuclei, on the other hand, have proven more challenging, and until recently the heaviest odd–odd $N = Z$ nucleus with a measured $B(E2; 2^+ \rightarrow 0^+)$ value was ^{58}Cu [12]. New efforts, however, are beginning to address this issue, with a measurement of the $B(E2; 2_1^+ \rightarrow 0_1^+)$ strength in ^{70}Br having been recently published [13]. Progress pushing beyond the $N = Z$ line is also being made, with recent measurements of the excited state energies in ^{70}Kr [14,15] and ^{74}Sr [16] allowing investigation of isospin symmetry breaking effects. Theoretical efforts are also making inroads in this mass region, with a study of isospin symmetry breaking and shape coexistence near mass $A \approx 70$ recently published [17].

In this letter, we report the measurement of the 2_1^+-state lifetime in the odd–odd $N = Z$ nucleus ^{74}Rb. This measurement extends the $B(E2)$ systematics of the odd–odd $N = Z$ nuclei and represents the heaviest such system with a measured 2_1^+-state lifetime. Previous studies of ^{74}Rb have established the level scheme up to spin-parity $J^\pi = 25^+$, with further tentative assignments up to $J^\pi = (31^+)$ [18–20]. Comparison with the level scheme of ^{74}Kr has allowed the identification of the $T = 1$ isobaric analogue states in ^{74}Rb up to $J^\pi = 8^+$ [20], a subset of which are shown in Fig. 1. Measurement of the 2_1^+-state lifetime in ^{74}Rb allows the $B(E2; 2_1^+ \rightarrow 0_1^+)$ transition strength to be deduced. This, in conjunction with the known analogue transition strength in ^{74}Kr, enables the decomposition of the isoscalar and isovector contributions to the transition strengths in the $A = 74, T = 1$ states [22,23]. While the isoscalar component is expected to dominate over the isovector, the degree to which this occurs is not necessarily obvious, as the increasing proximity of the $N = Z$ line to the proton drip line can introduce distortions to the wave functions or possibly lead to shape changes as discussed in, for example, Refs. [15,16]. In addition, ^{74}Kr exhibits strong shape coexistence, with its ground-state wave function composed of nearly equal contributions from intrinsic prolate and oblate configurations [7,24–26]. Comparison of the transition strength of ^{74}Kr with that measured here for ^{74}Rb can give an indication of whether such shape coexistence persists in ^{74}Rb, as the coexisting analogue 0_2^+ state has not been seen [20].

2. Differential Recoil Doppler Shift technique

For lifetimes in the range of a few picoseconds to about a nanosecond, the Recoil Distance Doppler Shift (RDDS) technique is often the experimental method of choice [27]. In this method, the distance between a nuclear reaction-inducing target and an energy-degrading (or stopping) foil must be varied to observe how the number of decays between the target and degrader changes. Only after data have been taken at several distances can the lifetime be determined reliably, which can necessitate long experiments. High production rates can offset the demanding data requirements, but for nuclei with low production rates the requisite beam time may become prohibitive. To address this problem, a variant of the RDDS technique called the Differential Recoil Distance Doppler Shift (DRDDS) method has been proposed [28,29]. This method modifies the traditional RDDS setup by inserting an additional energy-degrading foil between the target and the degrader. As a result, it is possible to measure the lifetime without systematic variation of the distance between the foils, significantly reducing the data required to measure the lifetime. A summary of the method is given below.

In both the RDDS and the DRDDS, the lifetime of an excited state is measured by determining the unnormalized decay function for that state $R(t)$ and its derivative:

$$R(t) = n_0 e^{-t/\tau}, \tag{1}$$

$$\frac{d}{dt}R(t) = -\frac{1}{\tau}R(t). \tag{2}$$

In the DRDDS, the three foils in the beam path cause the γ rays emitted by the excited reaction products to have three distinct Doppler-shifted components: a fast component from decays behind the target with an integral I_f, a reduced-velocity component behind the first degrader with integral I_r, and a slow component behind the second degrader with integral I_s. The decay function is the fraction of the beam that remains excited when it passes a given foil, e.g. $R(t_s) = I_s$. The derivative at the first degrader position can be approximated by

$$-\frac{dR}{dt} \approx \frac{R(t_r) - R(t_s)}{(t_s - t_r)} = \frac{(I_r + I_s) - I_s}{\Delta x / v} = I_r \frac{v}{\Delta x}, \tag{3}$$

where Δx is the distance and v is the beam velocity between the two degraders. Substituting these expressions in Eq. (2) and rearranging, the lifetime can be expressed as

$$\tau = \frac{\Delta x}{v}\frac{I_s}{I_r}. \tag{4}$$

In the DRDDS, all of these quantities can be directly measured from one distance setting for the two degraders.

Further discussion of the method is warranted in the case that the level of interest suffers from significant feeding from higher-lying states. A full discussion is given in Ref. [28], which can be summarized by stating that the effect of feeding is to delay the decay of the excited state which is being studied and causing an

excess of counts in the slow peak. It is possible to account for this effect by replacing I_s in Eq. (4) with $I_s - \sum_h b_h I_s^h$, where I_s^h is the slow component of the feeding state and b_h is the branching fraction from the feeding state to the state of interest. However, if the lifetime of the feeding state is short compared to the flight time between the target and first degrader, I_s^h approaches zero and the feeding does not affect the lifetime of interest. Because the DRDDS method does not make reference to the fast-peak population I_f, it is possible to choose the distance between the target and first degrader such that the feeding states have all decayed before reaching the first degrader. In this way, the fast peak serves as a buffer which isolates the reduced-velocity and slow peaks from the effects of feeding and reduces the sensitivity of the method to systematic uncertainties.

3. Experiment

The experiment was carried out at the National Superconducting Cyclotron Laboratory at Michigan State University. The Coupled Cyclotron Facility produced a primary beam of ^{78}Kr ions at an energy of 150 MeV/nucleon which was then impinged on a ^{9}Be target in order to induce nuclear reactions. The resulting beam was then purified in the A1900 fragment separator [30] with the aid of an aluminum degrader in order to select ^{74}Kr fragments after the target. The resulting secondary beam had a purity of about 40% ^{74}Kr with an energy of 93 MeV/nucleon and an average intensity of 1×10^5 particles per second.

The ^{74}Kr secondary beam was transported to the experimental area where the lifetime measurement was performed. This experiment used the TRIple PLunger for EXotic beams (TRIPLEX) [31], which was developed with the DRDDS method in mind and can hold up to three foils as targets or degraders/stoppers. The foils can be positioned between 0–25 mm apart using piezoelectric stepper motors. Three metallic foils were mounted in the TRIPLEX: one ^{9}Be target which was 139-mg/cm^2 thick, as well as two tantalum degraders of thickness 208 mg/cm^2 and 166 mg/cm^2. The ^{9}Be target was used to induce reactions in the secondary beam, which produced ^{74}Rb via the ^{9}Be(^{74}Kr, ^{74}Rb) charge-exchange reaction and excited ^{74}Kr through inelastic scattering, while the degraders were used to incrementally slow the reaction products to lower velocities. This approach avoids the difficulties associated with low beam intensity and purity which can pose a challenge to Coulomb excitation studies. The separations between the target/first degrader and first degrader/second degrader were 1 mm for the lifetime measurement, which corresponds to a flight-time of about 10 ps at a typical velocity of $\beta = 0.35$. Data were also taken with the target 10 mm from the first degrader to allow excited states to decay before reaching it. Any decays observed after the first degrader were then attributed to reactions induced in the degraders, which was found to be about 10% for ^{74}Kr and 20% for ^{74}Rb. The ratio of reactions happening in the first or second degrader was assumed to be the ratio of the degrader thicknesses.

The TRIPLEX was installed upstream of the S800 spectrograph [32]. Reaction residues observed in the focal plane of the S800 [33] were identified using the energy-loss vs time-of-flight method, with data taken for ^{74}Rb and ^{74}Kr simultaneously. The incoming beam was characterized by measuring its energy, y-position, and direction of travel at the target position as reconstructed by the S800 particle-tracking by taking data with neither target nor degraders installed. The energy loss of the beam through the target was measured with no degraders present, and then the degraders were installed to determine the energy loss through all three foils. The velocity v between the degraders (Eq. (4)) was calculated by taking the average energy measured in the S800 and correcting for the calculated energy loss in the second degrader.

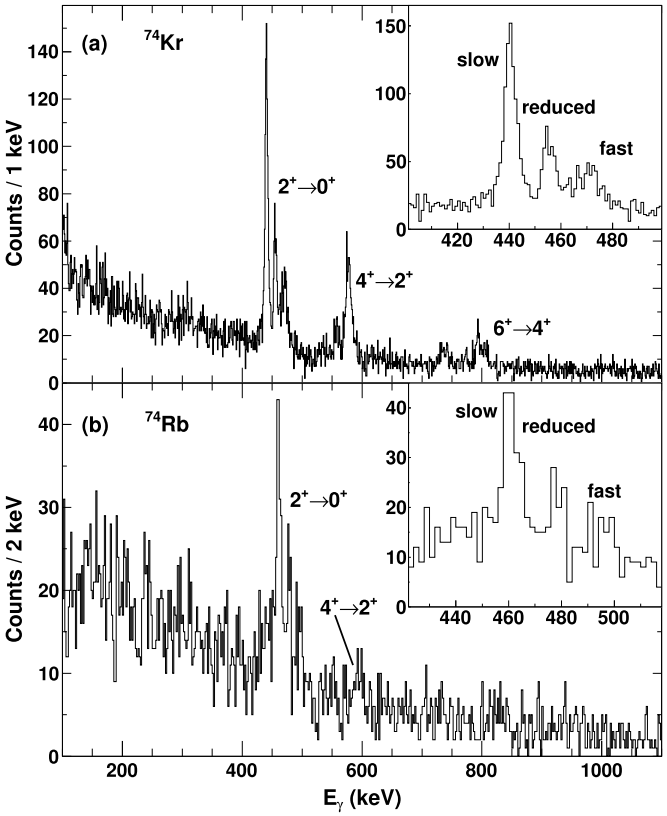

Fig. 2. Doppler-corrected γ-ray spectra detected in coincidence with (a) ^{74}Kr recoils and (b) ^{74}Rb recoils. For ^{74}Kr, several states are clearly populated, including the 2_1^+, 4_1^+, and 6_1^+ states. In contrast, only the 2_1^+ state is strongly populated in ^{74}Rb, with a small population of the 4_1^+ state visible. The insets show a closer view of the $2_1^+ \rightarrow 0_1^+$ transition for each nucleus, with the fast, reduced, and slow components labeled. The data in both panels were taken with 1 mm separations between the target/first degrader and between the first degrader/second degrader, and the Doppler correction was performed using the velocity after the first degrader.

De-excitation γ rays were detected in the Gamma Ray Energy Tracking In-beam Nuclear Array (GRETINA) [34]. For this experiment, GRETINA consisted of seven modules, each containing four 36-fold segmented high-purity germanium crystals. The TRIPLEX was mounted inside of GRETINA and shifted about 12 cm upstream of the center of the array. Accounting for the change in the target position, the array was configured with four detectors between 20°–50° and three detectors positioned around 70°. GRETINA was crucial to the success of this experiment due to its ability to localize γ-ray interaction points to within a few millimeters. The γ-ray position resolution of GRETINA, coupled with the particle-tracking of the S800, allows excellent Doppler-corrected energy resolution as described in Ref. [35]. Resolving three peaks for each transition has been a major challenge to the DRDDS [29], which is overcome by the combination of GRETINA and the S800. The spectra detected in coincidence with ^{74}Rb and ^{74}Kr recoils are shown in Fig. 2, with the transitions labeled by the initial and final states. The insets show the three components of the 2_1^+ states each labeled according to the velocity at which the photons are emitted. The velocity used for Doppler-reconstruction was the velocity after the first degrader, which was corrected event-by-event based on the energy measured in the S800. Therefore, the middle peak for each decay corresponds to the rest-frame γ-ray energy. Fig. 2 shows spectra for which the separation between the target/first degrader and first degrader/second degrader was 1 mm, which as mentioned earlier corresponds to a flight time of about 10 ps at a velocity of $\beta = 0.35$. Inspection of the spectra in Fig. 2 makes

it clear that the slow component of the 2^+ state is most strongly populated, indicating a lifetime significantly longer than 10 ps for both ^{74}Kr and ^{74}Rb.

The analysis of the lifetimes of the 2_1^+ states in ^{74}Kr and ^{74}Rb was performed with the aid of a Monte Carlo simulation program. Simulating the data addresses several issues, including the detector efficiency for each of the Doppler-shifted components, emission of photons within the foils, and evaluating the importance of feeding effects by including or excluding γ-ray cascades. The simulation package [36] is based on the Geant4 framework [37] and has been updated to include the GRETINA+TRIPLEX geometry. The software accepts several inputs which are used to reproduce the physical conditions measured during the experiment, including the beam properties described earlier, the momentum transfer during the reaction on target, and the acceptance of the S800 spectrograph. The simulation can also assign a fraction of the reactions to occur in the degraders instead of the target as determined in the analysis. Simulated γ-ray spectra were generated for the transitions observed in the data, with the lifetime of the 2_1^+ state varied systematically. The simulated spectra were then fit to the data in order to determine the 2_1^+-state lifetimes from a χ^2 minimization.

4. Analysis

The 2_1^+ state lifetime of ^{74}Kr was determined first to verify the performance of the DRDDS technique. Fig. 3(a) shows the results of fitting simulated decays from the 2_1^+ state to the ground state. Feeding from excited states was also included in this fit, which was fixed from the intensities of the higher-lying transitions as shown in Fig. 2. The shaded regions in this figure indicate the range used to determine the 2_1^+-state lifetime. It was found that about 30% of the $2_1^+ \rightarrow 0_1^+$ decays come from direct population of the 2_1^+ state, with the remaining population originating with feeding from the 4_1^+, 6_1^+, and 2_2^+ states. Simulations varying the lifetime of the 2_1^+ state were generated and fitted to the data, and the reduced χ^2 values from these fits were used to generate the χ^2 distribution shown in the inset of Fig. 3(a). The minimum of this distribution gives a lifetime of $\tau_{2_1^+} = 31(3)$ ps. The uncertainty includes both statistical and systematic contributions, with the main sources of systematic uncertainty being the positioning of the target and second degrader foils relative to the first degrader, as well as the position of the TRIPLEX relative to GRETINA. Each of these uncertainties contributes at about the 3% level. The sensitivity of the fit to the functional form used to describe the background was tested and found to be negligible. This result is in good agreement with the most precise published value of 33.8(6) ps, obtained with a differential-decay curve and recoil distance method [38]. It should be noted that these data were previously analyzed in Ref. [39] using a method based on a more standard RDDS technique, and was independently reanalyzed here with consistent results.

To evaluate the sensitivity of the DRDDS to feeding from short-lived states, the fitting procedure was repeated for ^{74}Kr without any feeding included in the simulations. The lifetime of the 4_1^+ state in ^{74}Kr is about 6 ps [39] and the higher-lying states are considerably shorter still [26,38], which satisfies the condition that the feeding lifetime should be shorter than the target-degrader flight-time. The results are shown in Fig. 3(b). The best-fit lifetime in this condition is $\tau_{2_1^+} = 33(3)$ ps, which includes systematic effects similar to the result which includes feeding. The 2 ps difference between the two fits to the ^{74}Kr data may be attributable to feeding; nevertheless, this result is consistent with that obtained when feeding is considered and also with the previously determined lifetime [38]. It should be noted that the fast peak is not reproduced well by the simulations in this case, which is a consequence of the lack of feeding transitions that would otherwise delay γ-ray emission and thereby reduce the population of this peak. However, since the fast peak is not explicitly considered in the DRDDS method, this does not alter the lifetime result.

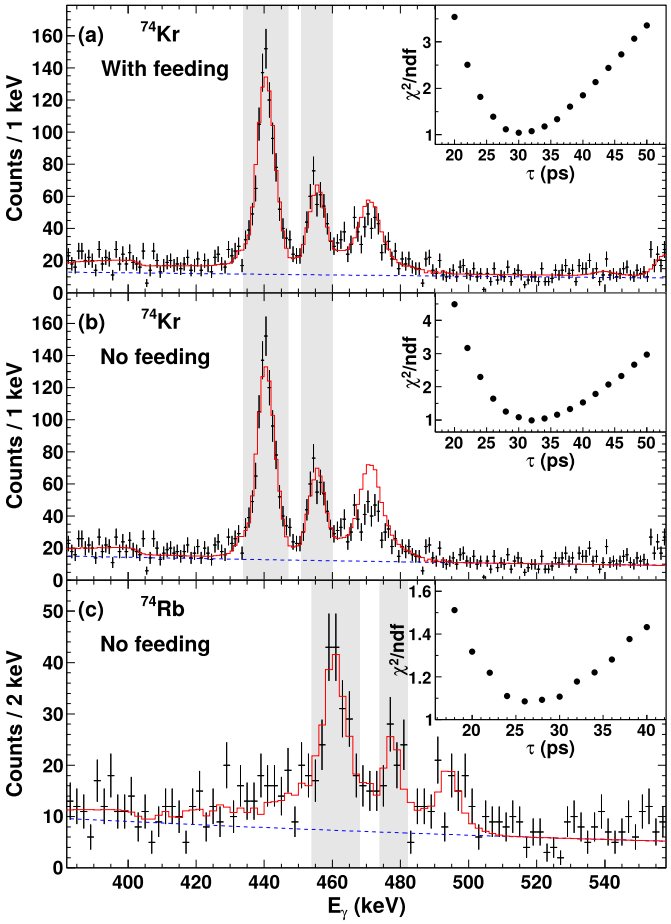

Fig. 3. Doppler-corrected γ-ray energy spectra for ^{74}Kr and ^{74}Rb along with the best-fit results of the 2_1^+-state lifetime for each nucleus. The data and uncertainties are indicated by the crosses, and the simulated spectra are shown by the solid lines. The shaded areas indicate the range used in the fits to determine the 2_1^+-state lifetime, and the exponential background is shown by the dashed line. Panel (a) shows the fit to the ^{74}Kr data including all observed feeding levels, while panel (b) shows the same fit when feeding is neglected (see text for details). Panel (c) shows the fit to the ^{74}Rb data. The insets show the reduced χ^2 distribution, the minimum of which was used to determine the lifetime.

The analysis of ^{74}Rb was performed in the same manner as ^{74}Kr. Feeding was neglected in this analysis, due both to the apparently little feeding from higher-lying states as well as lack of information on their lifetimes. As shown in Fig. 2, about 70% of the population goes to the 2^+ state in this reaction, with the remainder going to the 4^+ state. Although this state decays through a γ-ray with an energy of 575.1(4) keV [20], it apparently has a short lifetime and mostly populates the fast peak at approximately 600 keV. Since this lifetime is unknown, the insensitivity of the DRDDS technique to feeding from short-lived states is particularly important in this analysis. As with ^{74}Kr, simulations were generated for the $2_1^+ \rightarrow 0_1^+$ transition of ^{74}Rb, with the lifetime of the 2_1^+ state varied. These simulations were fitted to the data, with the resulting best fit shown in Fig. 3(c). The reduced χ^2 distribution is shown in the inset to this panel, and from the minimum of this distribution the lifetime was determined to be $\tau_{2^+} = 27(6)$ ps, which includes a small increase in the uncertainty to account for the fact that the reduced χ^2 does not go to one [40]. The uncer-

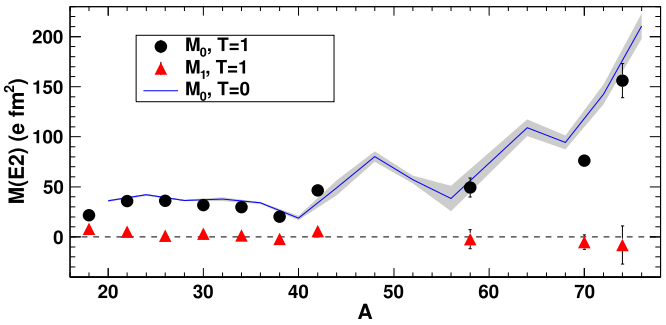

Fig. 4. $E2$ transition matrix elements decomposed into isoscalar and isovector components for a range of odd–odd ($T = 1$) nuclei. Isoscalar components are shown by black circles while isovector components are shown by red triangles. The isoscalar components of the matrix elements in the $T = 1$ triplets appear to dominate over the isovector components, which remain small and apparently flat within uncertainty. In addition, the M_0 appear to follow quite closely the matrix elements derived from even–even ($T = 0$) $N = Z$ nuclei, shown by the solid line. Data are from [4,11–13,23,41–53] and references therein.

tainty includes systematic effects similar to those in ^{74}Kr, and in addition includes a 6% contribution deduced from the difference between the two fits to the ^{74}Kr data to account for possible feeding. Assuming a lifetime for the 4^+ state similar to that in ^{74}Kr and including feeding in the simulations changes the lifetime by about 1 ps, which indicates that this is a reasonable estimate of the uncertainty from feeding from this state. An attempt was made to fit the 4_1^+ lifetime using the technique of Ref. [39], but the statistics are too low to achieve a reliable result. There is no evidence of decay from the $J^\pi = 3^+, T = 0$ state at 1005.4(3) keV, which would feed the 2_1^+ state via a 527.6(2)-keV γ ray [20]. Including simulations for decay from this state to the 2_1^+ state with lifetimes in the range 0–30 ps had no effect on the measured 2_1^+-state lifetime.

5. Discussion

From the lifetime, the reduced transition probability for the decay of the 2_1^+ state of ^{74}Rb can be calculated to be $B(E2; 2_1^+ \rightarrow 0_1^+) = 1.2(3) \times 10^3\ e^2\ \text{fm}^4$. Although the uncertainty is large due to the low statistics in the ^{74}Rb data, this value is comparable to that measured here for the analogue transition in ^{74}Kr, $B(E2; 2_1^+ \rightarrow 0_1^+) = 1.3(1) \times 10^3\ e^2\ \text{fm}^4$. This behavior is expected for transition properties among isobaric analogue states, as the structure of the states involved should be essentially equivalent under the assumption of isospin symmetry.

As mentioned in the introduction, the lowest-lying states in ^{74}Rb have been identified as members of the isospin $T = 1$ triplet in the $A = 74$ system. With the determination of the $B(E2; 2_1^+ \rightarrow 0_1^+)$ strength in ^{74}Rb and ^{74}Kr, it is possible to decompose the transition matrix elements for the $A = 74$, $T = 1$ states into isoscalar and isovector components, M_0 and M_1 respectively [22]. The relevant relation given in Ref. [22] can be written

$$\frac{1}{2}(M_0 - T_z M_1) = \sqrt{(2J_i + 1)B(E2; J_i \rightarrow J_f)}. \quad (5)$$

Based on Eq. (5), the $B(E2)$ from ^{74}Rb ($T_z = 0$) gives $M_0 = 2\sqrt{5B(E2; ^{74}\text{Rb})} = 160(20)\ e\ \text{fm}^2$. Then one can calculate the isovector contribution from $M_1 = M_0 - 2\sqrt{5B(E2; ^{74}\text{Kr})} = -10(20)\ e\ \text{fm}^2$. Notably, the isoscalar component of the matrix element dominates the transition strength, while the isovector part is consistent with zero.

The systematic behavior of the isoscalar and isovector contributions to the transition matrix elements is shown in Fig. 4 for a wide range of nuclei along the $N = Z$ line. For the $T = 1$ triplets, the isoscalar and isovector components of the matrix elements are plotted as black circles and red triangles, respectively. Although only three measurements are available for nuclei beyond mass $A = 42$, the isoscalar components of the matrix elements display a marked increase in the nuclei above the *sd* shell, in keeping with the observed increase in collectivity in this region. Notably, the isoscalar components of the matrix elements in the odd–odd nuclei follow very closely the evolution of the matrix elements derived from even–even $N = Z$ nuclei, shown by the solid line and error band in Fig. 4, which suggests that the collectivity in the $T = 0$ and $T = 1$ states has a common origin. This observation mirrors the findings of Ref. [54] based on an analysis of the energy systematics of $N = Z$ nuclei, in which it is found that $T = 1$ pairing is primarily responsible for collective excitations while $T = 0$ pairing results in single-particle characteristics. Further, the authors of that work propose that the ground states of even–even nuclei and the $T = 1$ states of neighboring odd–odd nuclei are both built on $T = 1$ coupling of nucleon pairs and thus have essentially the same correlation properties. The near identity of M_0 in neighboring species in Fig. 4 supports this interpretation.

In contrast to the isoscalar components of the matrix elements shown in Fig. 4, the isovector components show essentially no correlation with mass number. Furthermore, the isoscalar components of the matrix elements account for almost the entire transition strength, while the isovector components are consistent with zero. This suggests that the dominance of the isoscalar matrix elements in *sd*-shell nuclei may be a general property of nuclei on the $N = Z$ line, with no enhancement of the M_1 components up to $A = 74$. Specifically for $A = 74$, the fact that M_1 is consistent with zero serves as an indirect indicator of shape coexistence in ^{74}Rb. As mentioned in the introduction, the analogue of the 0_2^+ state that mixes with the ground state in ^{74}Kr has not been seen in ^{74}Rb, which makes direct determination of shape coexistence in this nucleus difficult. The small M_1 value indicates that there is no significant evolution between the $T_z = 1$ and $T_z = 0$ members of the $A = 74$ multiplet, such that ^{74}Rb and ^{74}Kr should exhibit the same degree of shape coexistence.

Finally, theoretical calculations continue to make progress in our understanding of this region, although they remain challenging [17,55]. The only theoretical prediction of the $B(E2)$ in ^{74}Rb of which the authors are aware is Ref. [56], in which shell model calculations of $N = Z$ nuclei between $A = 68$–76 have been performed. Although the authors of that study note that their calculated transition rates are too small due to truncations on their model space, they predict a rapid increase in collectivity starting at $A = 72$. They attribute this to occupation of the $g_{9/2}d_{5/2}$ orbitals, which drives a shape phase-transition between nuclei with $A \leq 70$ and $A > 70$. This predicted increase in collectivity is qualitatively in agreement with the trend observed in Fig. 4, and the overall trend in the predicted $B(E2)$ values matches the experimental data.

In summary, the lifetime of the 2_1^+ state in the odd–odd $N = Z$ nucleus ^{74}Rb has been measured. This was accomplished by using the Differential Recoil Distance Doppler-Shift method for the first time, demonstrating that it can be a valuable technique for measuring excited state lifetimes of exotic nuclei. The resulting $B(E2; 2_1^+ \rightarrow 0_1^+)$ in ^{74}Rb is consistent with that found between the isobaric analogue states in ^{74}Kr, as expected from isospin symmetry. Furthermore, the systematic dominance of the isoscalar over the isovector component of the transition matrix elements in nuclei beyond the *sd* shell is made clear and indicates that this may be a general trend. Finally, the $B(E2)$ value determined in this work suggests that ^{74}Rb may exhibit shape coexistence similar to ^{74}Kr, and merits further experiments in this regard.

This work is supported by the National Science Foundation (NSF) under PHY-1102511 and PHY-1565546, by the Department of Energy (DOE) National Nuclear Security Administration under Award No. DE-NA0000979, by the UK STFC, and partly by BMBF (Germany) under Contract No. 05P12PKFNE. This material is based upon work supported by the U.S. Department of Energy, Office of Science, Office of Nuclear Physics under Contracts No. DE-AC02-05CH11231 (LBNL). GRETINA was funded by the US DOE—Office of Science and operation of the array at NSCL is supported by NSF under Cooperative Agreement PHY-1102511 (NSCL) and DOE under Grant No. DE-AC02-05CH11231 (LBNL). C. M. would like to thank A. O. Macchiavelli for very enlightening discussions.

References

[1] M.A. Bentley, S.M. Lenzi, Prog. Part. Nucl. Phys. 59 (2007) 497.
[2] J.C. Hardy, I.S. Towner, Phys. Rev. C 91 (2015) 025501.
[3] M. Girod, J.P. Delaroche, A. Görgen, A. Obertelli, Phys. Lett. B 676 (2009) 39.
[4] K. Starosta, et al., Phys. Rev. Lett. 99 (2007) 042503.
[5] A. Obertelli, et al., Phys. Rev. C 80 (2009) 031304.
[6] A. Gade, et al., Phys. Rev. Lett. 95 (2005) 022502.
[7] E. Bouchez, et al., Phys. Rev. Lett. 90 (2003) 082502.
[8] W. Nazarewicz, J. Dudek, R. Bengtsson, T. Bengtsson, I. Ragnarsson, Nucl. Phys. A 435 (1985) 397.
[9] S.M. Fischer, D.P. Balamuth, P.A. Hausladen, C.J. Lister, M.P. Carpenter, D. Seweryniak, J. Schwartz, Phys. Rev. Lett. 84 (2000) 4064.
[10] J.H. Hamilton, et al., Phys. Rev. Lett. 32 (1974) 239.
[11] A. Lemasson, et al., Phys. Rev. C 85 (2012) 041303.
[12] A.F. Lisetskiy, et al., Phys. Rev. C 68 (2003) 034316.
[13] A. Nichols, et al., Phys. Lett. B 733 (2014) 52.
[14] D.M. Debenham, et al., Phys. Rev. C 94 (2016) 054311.
[15] K. Wimmer, et al., Phys. Lett. B 785 (2018) 441.
[16] J. Henderson, et al., Phys. Rev. C 90 (2014) 051303.
[17] A. Petrovici, Phys. Rev. C 91 (2015) 014302.
[18] D. Rudolph, et al., Phys. Rev. Lett. 76 (1996) 376.
[19] C.D. O'Leary, et al., Phys. Rev. C 67 (2003) 021301.
[20] S.M. Fischer, et al., Phys. Rev. C 74 (2006) 054304.
[21] B. Singh, A.R. Farhan, Nucl. Data Sheets 107 (2006) 1923.
[22] A.M. Bernstein, V.R. Brown, V.A. Madsen, Phys. Rev. Lett. 42 (1979) 425.
[23] P.D. Cottle, AIP Conf. Proc. 638 (2002) 37.
[24] C. Chandler, et al., Phys. Rev. C 56 (1997) R2924.
[25] F. Becker, et al., Eur. Phys. J. A 4 (1999) 103.
[26] E. Clément, et al., Phys. Rev. C 75 (2007) 054313.
[27] P.J. Nolan, J.F. Sharpey-Schafer, Rep. Prog. Phys. 42 (1979) 1.
[28] A. Dewald, S. Harissopulos, P. von Brentano, Z. Phys. A 334 (1989) 163.
[29] A. Dewald, O. Möller, P. Petkov, Prog. Part. Nucl. Phys. 67 (2012) 786.
[30] D.J. Morrissey, et al., Nucl. Instrum. Methods Phys. Res., Sect. B 204 (2003) 90.
[31] H. Iwasaki, et al., Nucl. Instrum. Methods Phys. Res., Sect. A 806 (2016) 123.
[32] D. Bazin, et al., Nucl. Instrum. Methods Phys. Res., Sect. B 204 (2003) 629.
[33] J. Yurkon, D. Bazin, W. Benenson, D. Morrissey, B. Sherrill, D. Swan, R. Swanson, Nucl. Instrum. Methods Phys. Res., Sect. A 422 (1999) 291–295.
[34] S. Paschalis, et al., Nucl. Instrum. Methods Phys. Res., Sect. A 709 (2013) 44.
[35] D. Weisshaar, et al., Nucl. Instrum. Methods Phys. Res., Sect. A 847 (2017) 187.
[36] P. Adrich, et al., Nucl. Instrum. Methods Phys. Res., Sect. A 598 (2009) 454.
[37] S. Agostinelli, et al., Nucl. Instrum. Methods Phys. Res., Sect. A 506 (2003) 250.
[38] A. Görgen, et al., Eur. Phys. J. A 26 (2005) 153.
[39] H. Iwasaki, et al., Phys. Rev. Lett. 112 (2014) 142502.
[40] C. Patrignani, P.D. Group, Chin. Phys. C 40 (2016) 100001.
[41] D.R. Tilley, C.M. Cheves, J.H. Kelley, S. Raman, H.R. Weller, Nucl. Phys. A 636 (1998) 249.
[42] R.B. Firestone, Nucl. Data Sheets 108 (2007) 2319.
[43] M.S. Basunia, Nucl. Data Sheets 114 (2013) 1189.
[44] C. Ouellet, B. Singh, Nucl. Data Sheets 112 (2011) 2199.
[45] N. Nica, J. Cameron, B. Singh, Nucl. Data Sheets 113 (2012) 1.
[46] J. Chen, Nucl. Data Sheets 140 (2017) 1.
[47] J. Chen, B. Singh, J.A. Cameron, Nucl. Data Sheets 112 (2011) 2357.
[48] T.W. Burrows, Nucl. Data Sheets 107 (2006) 1747.
[49] Y. Dong, H. Junde, Nucl. Data Sheets 128 (2015) 185.
[50] H. Junde, H. Su, Y. Dong, Nucl. Data Sheets 112 (2011) 1513.
[51] E.A. McCutchan, Nucl. Data Sheets 113 (2012) 1735.
[52] D. Abriola, A.A. Sonzogni, Nucl. Data Sheets 111 (2010) 1.
[53] J.N. Orce, et al., Phys. Rev. C 77 (2008) 064301.
[54] A. Macchiavelli, et al., Phys. Lett. B 480 (2000) 1.
[55] A.P. Zuker, A. Poves, F. Nowacki, S.M. Lenzi, Phys. Rev. C 92 (2015) 024320.
[56] M. Hasegawa, K. Kaneko, T. Mizusaki, Y. Sun, Phys. Lett. B 656 (2007) 51.